Multirate Attitude Control of Dual-rotor System Considering Propeller Loss of Effectiveness

Binh-Minh Nguyen, Sakahisa Nagai and Hiroshi Fujimoto
Department of Advanced Energy
The University of Tokyo
corresponding author's e-mail: nguyen.binhminh@edu.k.u-tokyo.ac.jp

***Abstract*—This paper presents a two-degree-of-freedom control system for improving the attitude control performance under the existence of propeller's loss of effectiveness (LoE). To deal with the long sampling time of attitude measurements, a multirate observer is designed to estimate the attitudes at every control period of the propeller actuator. Using the estimated attitudes, the LoEs are identified via recursive least squares (RLS) algorithm. Using the identified LoEs, the propeller speed references are adjusted to compensate the fault effect on the system. Some physical parameters of the attitude dynamics are also identified to adaptively update the feedforward controller. In summary, the proposed system only consists of practical algorithms which can be implemented conveniently in real applications. Experiments using a dual-rotor testbench show that the proposed system can quickly identify the time-varying LoEs. In comparison with a conventional singlerate control system without fault tolerance, the proposed system can reduce the pitch angle and yaw angle tracking errors by 69.3 % and 39.6 %, respectively.**

Keywords— adaptive feedforward, fault identification, multi-rate control, multi-rotor, recursive least square.

I. INTRODUCTION

Multi-rotors have been shown promising tools in many fields of human society [1]. To maintain the safe and stable motion of multi-rotors, it is essential to control not only the altitude [2] but also the attitude. To guarantee good attitude control performance, the following issues are indispensable.

The first issue is the propeller's loss of effectiveness (LoE). As demonstrated in Fig. 1(a), LoE happens as the actual thrust deviates from the desired value. If the LoE was not detected and compensated, unwanted moments might be generated. This might consequently deteriorates the attitudes tracking performance. To quantitatively estimate the LoE fault, state estimation approaches have been studied [3] - [10]. However, these works commonly treated the LoE fault as an augmented state α of the system dynamics. This increases the size of the state space model and the computational effort. Moreover, the augmented system is nonlinear due to the multiplicity $(1-\alpha)u$, where u is the system input. Although the extended Kalman filter is applicable, it requires the Jacobian matrix calculation at every control period [3]. The adaptive exogeneous Kalman filter [4], the PI observer [5], and the robust observer [6] requires the linearization process. Besides, it might take few seconds to estimate the fault by the aforementioned methods [3] – [10]. As shown in Fig. 1(b), the fault is only detected about one second after it occurs [10]. It also takes about three seconds for the estimated fault to reasonably approximate the true magnitude. Some previous studies utilized the motor current [8] or propeller speed sensors [9]. Unfortunately, such sensors are not always available on the commercial multi-rotors, especially the small-scale drones.

The second issue is the sampling mismatch in the system. The control period of propeller actuators is commonly much shorter than that of the attitude measurements. It is well known that good tracking performance cannot be achieved if we directly feedback the long-sampling-time measurement. However, this issue has not been investigated in the literature of multi-rotor motion control. The works [3] - [10] merely utilized the continuous model or the discrete model with single-sampling-time.

This paper presents an attitude control system that simultaneously addressing the aforementioned discussions. The proposal of this paper was motivated by the adaptive robust control of multi-sampling time systems with the application to linear motors [11] and machine tool [12]. For the sake of safety when conducting experiment, this paper uses a dual-rotor testbench. The system can imitates the yaw and pitch motion of the real multi-rotors. This paper assumes that the motor drives have enough capacity to compensate the faults. The proposed control system consists of the two-degree-of-freedom controller (2DOFC), the multirate observer (MROB), and the recursive least square (RLS) parameter identification. The MROB is to perform the sensor fusion of attitude measurements (yaw, pitch) with the inertia measurement unit (yaw-rate, pitch-rate). The MROB outputs the estimated attitudes at every period of the propeller actuator control. The estimated attitudes are used to identify the LoEs and some uncertain parameters of the attitude dynamics via RLS algorithm. Fault compensation is realized by adjusting the propeller speed references. Furthermore, the feedforward controller is adaptively updated using the identified parameters. For the sake of paper space, this paper only focuses on the estimation and identification algorithm. For the purpose of system design and analysis, we have proposed several approaches by using circle criterion [2] and generalized frequency variable [13].

The reminder of this paper is organized as follows. The model of the test-bench under study is presented in Section 2. The proposed system is presented in Section 3, followed by the validation results in Section 4. Finally, the conclusions are stated in Section 5.

II. MODELING OF THE TESTBENCH

The model of testbench system is shown in Fig. 2. It has two propellers driven by direct current motors. The main specification of the system is shown in Table 1. In Fig. 2, θ

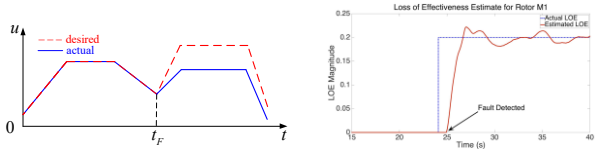

(a) LoE happens since t_F. (b) LoE identification in [10].

Fig. 1. LoE: a typical propeller actuator fault.

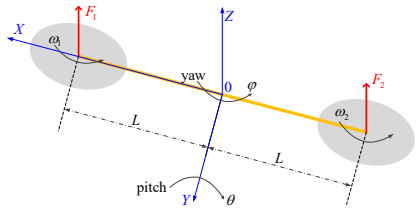

Fig. 2. Model of testbench system in half-quadrotor mode.

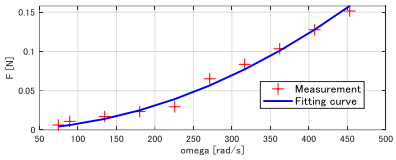

Fig. 3. Thrust characteristics of the propeller.

TABLE I. DESCRIPTION OF TESTBENCH

Operating space	$52cm \times 52cm \times 62cm$
Pitch encoder resolution	2880 counts/revolution
Yaw encoder resolution	4096 counts/revolution
Inertial measurement unit (IMU)	IIM-42652 6-Axis MEMS
Thrust displacement	$L = 0.158\ m$
Pitch moment constant S_p	$5 \times 10^{-5} N.m.s.rad^{-1}$
Yaw moment constant S_y	$10 \times 10^{-5} N.m.s.rad^{-1}$
Thrust constant C	$7.7 \times 10^{-7}\ N.rad^{-2}.s^{-2}$

and φ denote the pitch and yaw angles, respectively. Their rates and accelerations are denoted by $v_{\theta(\varphi)}$ and $a_{\theta(\varphi)}$, respectively. The pitch and yaw motions are described as

$$J_p a_\theta + D_p v_\theta + K_p \theta = M_p;\ J_y a_\varphi + D_y v_\varphi + K_y \varphi = M_y \quad (1)$$

where $J_\#$, $D_\#$ and $K_\#$ are the moment of inertia, damping, and stiffness ($\# = \{p, y\}$). The moments $M_\#$ are generated by the thrusts. As shown in Fig. 3, the thrust is characterized as $F_i = C\omega_i^2$. Since the motor speed control loop is relatively fast, ω_i is reasonably approximated by its reference ω_i^*. Linearizing the thrust characteristics, $M_\#$ can be expressed as

$$M_p = S_p\omega_1^* - S_p\omega_2^*;\ M_y = S_y\omega_1^* + S_y\omega_2^* \quad (2)$$

where the moment constant $S_\#$ are given in Table 1.

Fig. 4 describes the conventional attitude control system with the feedback controllers $C_{fb,p(y)}$, the holder $\mathcal{H}$ and the sampler $\mathcal{S}$. Let T_{yl} and T_{yh} be the sampling times of the attitudes and their rates, respectively. The pitch-rate and yaw-rate can be measured directly using the inertia measurement unit (IMU). However, the attitudes are not measured directly. They are commonly obtained from some "virtual sensors" with the signal processing process. Typical examples are on-board vision system or global positioning system (GPS). Due to the required time for signal processing, T_{yl} is usually much longer than T_{yh}. As shown in Fig. 5, it is assumed that $T_r = T_u = T_{yh} = T_{yl}/N$ where N is an integer ($N \geq 2$). Here, T_r is the period to generate the attitude reference, and T_u is the period of propeller speed control. From (2), the reference speeds of the motor drives are calculated as follows

$$\omega_1^* = \frac{M_p^*}{2S_p} + \frac{M_y^*}{2S_y};\ \omega_2^* = \frac{-M_p^*}{2S_p} + \frac{M_y^*}{2S_y} \quad (3)$$

III. PROPOSED CONTROL SYSTEM

A. Problem Setting

If the propellers lost their effectiveness, the actual thrusts and the moment $M_\#$ deviate from the desired values. Defining the LoE of the propeller i as the variable $\alpha_i \in [0, 1]$. Under the existence of LoEs, the pitch and yaw moments become

$$\begin{cases} M_p = S_p\omega_1^*(1-\alpha_1) - S_p\omega_2^*(1-\alpha_2) \\ M_y = S_y\omega_1^*(1-\alpha_1) + S_y\omega_2^*(1-\alpha_2) \end{cases} \quad (4)$$

Using the inputs $\omega_{1,2}^*$ and the outputs $\theta, v_\theta, \varphi, v_\varphi$, this paper aims to improve the performance of the conventional control system in Fig. 4 by estimating the LoEs $\alpha_{1,2}$, the states θ, φ, and the parameters $J_\#, D_\#$ and $K_\#$ at every fundamental period $T_s = T_r = T_u = T_{yh}$. Unlike the conventional feedback control system, the proposed system in Fig. 6 includes the multirate estimator, the adaptive moment-to-speed transformation, and the adaptive feedforward controllers $C_{ff,\#}$. In summary, the proposed system is a type of direct adaptive control system. By using the stable desired poles to design the feedback controllers and setting upper-bound and lower-bound for the identified parameters, it is possible to guarantee the convergence of the attitude angles to their reference values. This can be guaranteed even if the identified parameters do not converge.

B. Multirate estimator

Fig. 7 describes the configuration of the proposed multirate estimator, which includes the state observer (SoB), the LoE Identification (LoE-ID), and the parameter identification (PR-ID).

SoB: From (1), the following discrete model is established with the fundamental sampling time T_s:

$$\begin{cases} x_{\#(k+1)} = A_{\#(k)}x_{\#(k)} + B_{\#(k)}u_{\#(k)} \\ y_{\#(k)} = C_{\#(k)}x_{\#(k)} \end{cases} \quad (5)$$

where k denotes the time stamp. The state and input vectors are defined as $x_{p(k)} = \left[v_{\theta(k)}\ \theta_{(k)}\right]^{\mathrm{T}}, u_{p(k)} = M_{p(k)}$; and $x_{y(k)} = \left[v_{\varphi(k)}\ \varphi_{(k)}\right]^{\mathrm{T}}, u_{y(k)} = M_{y(k)}$. Assuming that T_s is short enough, the state matrix and input matrix are calculated as follows with the 2×2 identity matrix I_2

$$A_\# = \mathrm{I}_2 + T_s\begin{bmatrix} -D_\#/J_\# & -K_{s\#}/J_\# \\ 1 & 0 \end{bmatrix}, B_\# = T_s\begin{bmatrix} 1/J_\# \\ 0 \end{bmatrix} \quad (6)$$

and the output $y_{p(k)}$ consists of the pitch-rate and pitch angle measurement; the output $y_{y(k)}$ consists of the yaw-rate and yaw angle measurement. Thus, the switching of the output matrix is expressed as

$$C_{\#(k)} = \begin{bmatrix} 1 & 0 \\ 0 & c_{22} \end{bmatrix}, c_{21} = \begin{cases} 1 & \text{if the attitude is updated} \\ 0 & \text{during the inter-samples} \end{cases} \quad (7)$$

The state variables are estimated as

$$\hat{x}_{\#(k+1)} = A_\#\hat{x}_{\#(k)} + B_\#u_{\#(k)} + L_{o\#(k)}\left(y_{\#(k)} - C_{\#(k)}\hat{x}_{\#(k)}\right) \quad (8)$$

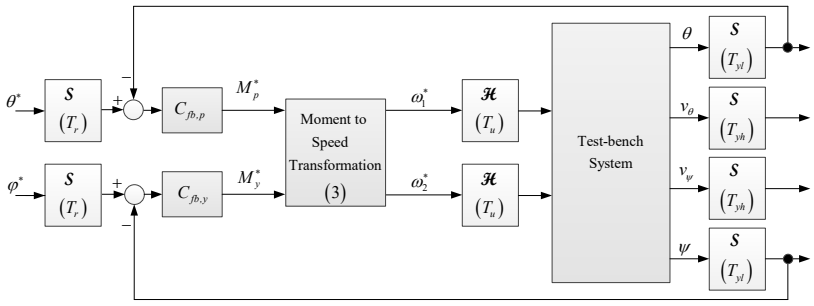

Fig. 4. Conventional attitude control system.

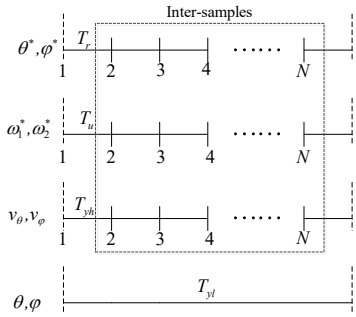

Fig. 5. Multi-samplings of the system.

In (8), the matrices $A_{\#}, B_{\#}$ are updated at every control period using the identified values of $J_{\#}$, $D_{\#}$ and $K_{\#}$. The observer gain matrix $L_{o\#(k)}$ is designed using pole-placement to the pair of $\{A_{\#}, C_{\#(k)}\}$. During the inter-samples, the states are only corrected by using the available measurement of IMU [14]. This means the elements of $L_{o\#(k)}$ associated with the attitude measurement are set to be zero during inter-samples. The pitch and yaw moment are updated by using the identified LoEs and the propeller speed references:

$$\begin{cases} M_{p(k)} = S_p\omega_{1(k)}^{*}\left(1-\alpha_{1(k)}\right) - S_p\omega_{2(k)}^{*}\left(1-\alpha_{2(k)}\right) \\ M_{y(k)} = S_y\omega_{1(k)}^{*}\left(1-\alpha_{1(k)}\right) + S_y\omega_{2(k)}^{*}\left(1-\alpha_{2(k)}\right) \end{cases} \quad (9)$$

PR-ID: From (1), the following relationship is derived

$$\mathrm{Y}_{\#(k)} = \Phi_{\#(k)}^{\mathrm{T}}\Theta_{\#(k)} \quad (10)$$

where $\mathrm{Y}_{p(k)} = M_p$, $\mathrm{Y}_{y(k)} = M_{y(k)}$ and

$$\Phi_{p(k)}^{\mathrm{T}} = \begin{bmatrix} a_{\theta(k)} & v_{\theta(k)} & \theta_{(k)} \end{bmatrix},\ \Phi_{y(k)}^{\mathrm{T}} = \begin{bmatrix} a_{\varphi(k)} & v_{\varphi(k)} & \varphi_{(k)} \end{bmatrix},$$
$$\Theta_{\#(k)} = \begin{bmatrix} J_{\#(k)} & D_{\#(k)} & K_{\#(k)} \end{bmatrix}^{\mathrm{T}}$$

The RLS algorithm that estimating the parameters is described as follows [11]

$$\hat{\Theta}_{\#(k)} = \hat{\Theta}_{\#(k-1)} + \mathrm{L}_{Id\,\#(k)}\left(\mathrm{Y}_{\#(k)} - \Phi_{\#(k)}^{\mathrm{T}}\hat{\Theta}_{\#(k-1)}\right)$$
$$\mathrm{L}_{Id\,\#(k)} = \mathrm{P}_{\#(k-1)}\Phi_{\#(k)}\left(\vartheta\mathrm{I} + \Phi_{\#(k)}^{\mathrm{T}}\mathrm{P}_{\#(k-1)}\Phi_{\#(k)}\right)^{-1}$$
$$\mathrm{P}_{\#(k)} = \frac{1}{\vartheta}\left(\mathrm{I} - \mathrm{L}_{Id\,\#(k)}\Phi_{\#(k)}^{\mathrm{T}}\right)\mathrm{P}_{\#(k-1)}$$

where I_3 is the 3×3 identity matrix, $\mathrm{L}_{Id\#(k)}$ is the identification gain, and $\mathrm{P}_{\#(k)}$ is the covariance matrix. The forgetting factor ϑ is chosen as a positive constant slightly smaller than one. Matrix $\Phi_{\#(k)}^{\mathrm{T}}$ is updated by the estimated values of the state observers. If the persistent excitation (PE) condition is not satisfied, no update is performed and $P_{\#(k)} = P_{\#(k-1)}$ [15]. The values $a_{\theta(k)}$ and $a_{\varphi(k)}$ are calculated using the estimated values of $v_\theta[k]$ and $v_\varphi[k]$, respectively.

$$a_{\theta(k)} = \left(v_{\theta(k)} - v_{\theta(k-1)}\right)\Big/T_s,\ a_{\varphi(k)} = \left(v_{\varphi(k)} - v_{\varphi(k-1)}\right)\Big/T_s \quad (11)$$

LoE-ID: Let $\beta_i = 1 - \alpha_i$ ($i = 1, 2$). The following relationship is formulated from (1) and (4)

$$\mathrm{Y}_{loe(k)} = \Phi_{loe(k)}^{\mathrm{T}}\Theta_{loe(k)} \quad (12)$$

where

$$\Theta_{loe(k)} = \begin{bmatrix} \beta_{1(k)} & \beta_{2(k)} \end{bmatrix}^{\mathrm{T}},\ \Phi_{loe(k)}^{\mathrm{T}} = \begin{bmatrix} S_\theta\omega_1^{*} & -S_\theta\omega_1^{*} \\ S_\varphi\omega_1^{*} & S_\varphi\omega_2^{*} \end{bmatrix}$$
$$\mathrm{Y}_{loe(k)} = \begin{bmatrix} J_p a_{\theta(k)} + D_p v_{\theta(k)} + K_p\theta_{(k)} \\ J_y a_{\varphi(k)} + D_y v_{\varphi(k)} + K_y\varphi_{(k)} \end{bmatrix}$$

From (12), the LoE values can be identified using the RLS algorithm which is similar to that of the PR-ID. Note that, $\mathrm{Y}_{loe(k)}$ is updated using the estimated values sent from SoB and PR-ID. In summary, the SOB, LoE-ID and PR-ID shares their estimated values with each other. This adaptive estimation configuration has been applied to some practical applications, such as simultaneous estimation of sideslip angle and cornering stiffness for electric vehicle motion control [16].

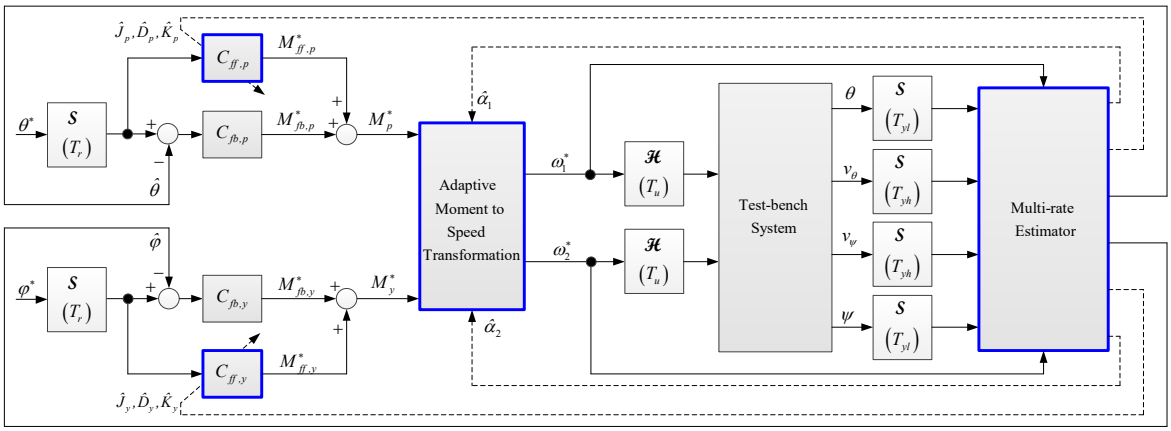

Fig. 6. Proposed multirate attitude control system.

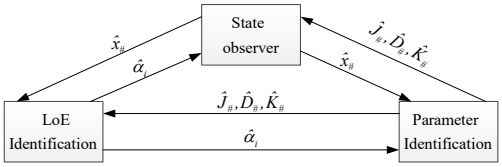

Fig. 7. Configuration of the proposed multirate estimator.

C. Adaptive feedforward control

Given the reference signals θ^* and φ^*, the feedforward control signals are updated as follows

$$\begin{cases} M^*_{ff,p(k)} = \hat{J}_{p(k)} a^*_{\theta(k)} + \hat{D}_{p(k)} v^*_{\theta(k)} + \hat{K}_{p(k)} \theta^*_{(k)} \\ M^*_{ff,y(k)} = \hat{J}_{y(k)} \dot{v}^*_{\varphi(k)} + \hat{D}_{y(k)} v^*_{\varphi(k)} + \hat{K}_{y(k)} \varphi^*_{(k)} \end{cases} \quad (13)$$

D. Adaptive moment to speed transformation

Let $\omega_{min,(max)}$ be the minimum (maximum) speed of the propeller, respectively; and define the limitation function as

$$f_{\text{limit}}(\omega) = \begin{cases} \omega_{\max} : \text{if } \omega \geq \omega_{\max} \\ \omega : \quad \text{if } \omega_{\min} < \omega < \omega_{\max} \\ \omega_{\min} : \text{if } \omega \leq \omega_{\min} \end{cases} \quad (14)$$

If the LoE appears in a propeller, its speed should be increased to satisfy the required moments of the pitch and yaw motion controllers. However, the speed of the propeller must not exceed its minimum and maximum values. In summary, the reference speeds in Fig. 7 is calculated as follows

$$\omega^*_{1(k)} = f_{\text{limit}}\left(\left(\frac{M^*_{p(k)}}{2S_\theta} + \frac{M^*_{y(k)}}{2S_\varphi}\right)\frac{1}{1-\hat{\alpha}_{1(k)}}\right) \quad (15)$$

$$\omega^*_{2(k)} = f_{\text{limit}}\left(\left(\frac{-M^*_{p(k)}}{2S_\theta} + \frac{M^*_{y(k)}}{2S_\varphi}\right)\frac{1}{1-\hat{\alpha}_{2(k)}}\right) \quad (16)$$

IV. Evaluation

A. Experimental setting

The experimental system is shown in Fig. 8. By using the QUARC platform provided by Quanser, the control system is implemented in Matlab/Simulink. To imitate the actual multi-rotor system, the sampling times of the pitch and yaw angle are set as 500 milliseconds in the testbench experiment. The sampling times of the yaw-rate and pitch-rate are set as 1 millisecond, which is also the control period of the motor drives. To evaluate the proposed system, two tests were performed. The first test is to validate the multirate estimator. The second test is to validate the overall control system. The control gains are obtained via pole-placement with respect to the nominal dynamics (1). The poles of the closed-loop system including $C_{fb,p}$ and the pitch dynamics are placed at -0.9. The poles of the closed-loop system including $C_{fb,y}$ and the yaw dynamics are placed at -1.1. The nominal parameters are set as follows

$$J_{p,y} = \{0.0220, 0.0140\}\ [kg.m^2],$$
$$D_{p,y} = \{0.0077, 0.0300\}\ [N.m.s.rad^{-1}],$$
$$K_{p,y} = \{0.0380, 0.0250\}\ [N.m.rad^{-1}].$$

The poles of the SoB are chosen as $\{-120, -40\}$. The forgetting factors are chosen as 0.999 for the PR-ID, and 0.999 for the LoE-ID. The experimental time is 120 seconds.

B. Test 1: Validation of the multi-rate estimator

The identified values of LoEs and the parameters are shown in Figs. 9 and 10, respectively. As described belows, three test cases were conducted for comparison.

Test 1A (Fig. 9(a)): The LoEs were identified by directly using the measurement of the IMU and the low-rate attitudes. The parameters $J_\#$, $D_\#$ and $K_\#$ were fixed as the nominal values shown in the previous subsection.

Fig. 8. Experimental system.

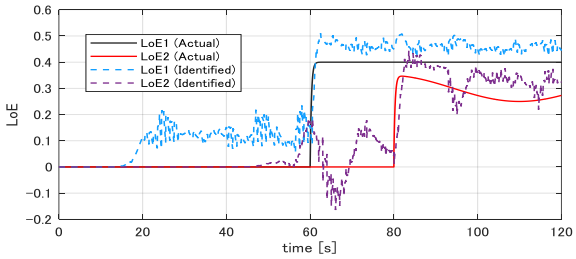

(a) Test 1A

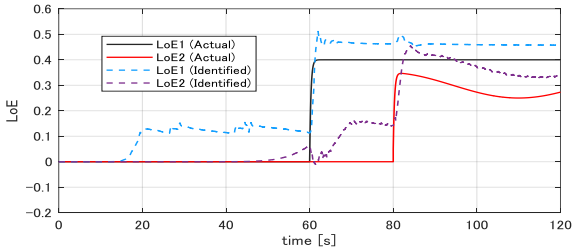

(b) Test 1B

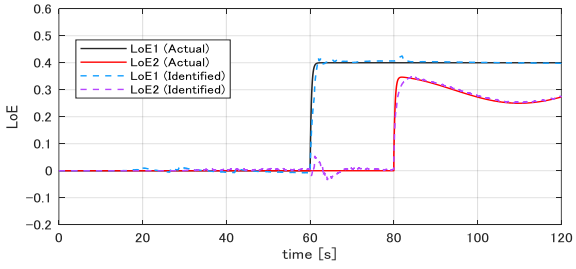

(c) Test 1C

Fig. 9. Test 1: LoE estimation result.

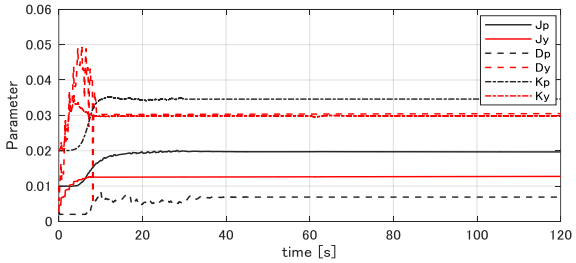

Fig. 10. Identified parameters in Test 1.

Test 1B (Fig. 9(b)): The LoEs were identified by using the estimated values of the SoB. However, the physical parameters were fixed as in Test 1B.

Test 1C (Fig. 9(c)): The LoEs were identified by the proposed multirate estimator. This means, the physical parameters were adaptively updated in real-time. The identified parameters were shown in Fig. 9.

Thanks to the state observer, the results of Test 1B were smoothly improved in comparison with Test 1A which directly used the long sampling time attitude measurements. However, the results of Tests 1A and 1B were considerably influenced by the model uncertainty. By adaptively estimating the state and physical parameters, the system in Test 1C can quickly identify the LoEs. This fault detection is much faster than that shown in Fig. 1(b) [10].

C. Test 2: Validation of the overall control system

Four test cases were performed as follows:

Test 2A: The conventional control system in Fig. 4.

Test 2B: Although the multi-rate observer is implemented to provide the estimated attitudes at high-rate, the LoE compensation and feedforward controller are not utilized.

Test 2C: The system is almost similar to the proposed system Fig. 6 except the feedforward controller.

Test 2D: The proposed control system in Fig. 6.

Unlike almost the existing studies which merely considered the LoE as a simple step signal (Fig. 1(b)), this study examined the LoE pattern shown in Fig. 11. As shown in Fig. 11, propeller 2 is always healthy while propeller 1 suddenly suffers a time-varying LoE α_1 since 60 seconds. The latency of sensors [14] is not investigated, as it is not the main goal of this paper.

The results of Test 2A are shown in Fig. 12. Due to the feedback of the long sampling time measurements, the system had to experience a noticeable vibration of the pitch angle and yaw angle. Moreover, the attitude tracking performance was considerably degraded due to the LoE since 60 seconds. The results of Test 2B are demonstrated in Fig. 13. By utilizing the multirate observer, the feedback controllers was provided with the high-rate and smooth estimated attitudes. Consequently, the control performance was improved. Especially, Test 2B did not experience the attitude vibration as in Test 2A. Next, the results of Test 2C are shown in Fig. 14. Thanks to the multirate observer and the compensation of the LoEs, the attitude tracking performance was remarkably improved in comparison with Tests 2A and 2B. Finally, the results of Test 2D are shown in Fig. 15. This test case attained the best tracking performance, as the feedforward controller was adaptively updated.

For thoroughly evaluating four test cases, root-mean-square-deviation (RMSD) of the tracking errors are summarized in Table 2. It can be seen that, in comparison with Test 2A, the RMSD values of pitch and yaw tracking errors are respectively reduced 69.3% and 39.6% by the proposed system in Test 2D.

V. CONCLUSIONS

This paper proposed a multirate adaptive control system for improving the attitude performance of multi-rotors under the existence of propeller's LoE. The proposed system was developed by practical RLS algorithms, which allow it to be implemented quickly and conveniently in real applications. The effectiveness of the proposed system has been evaluated by real-time experiments. The necessity of multirate control with adaptive feedforward and LoE identification has been proved by using a dual-rotor testbench. In future, the proposed system will be further improved to deal with the external disturbances and the latency of sensor measurements. The implementation of the proposed method to a real multi-rotor is another goal of this study.

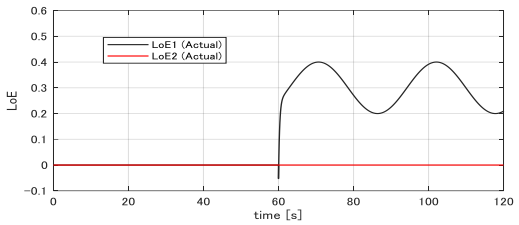

Fig. 11. LoE pattern in Test 2.

TABLE II. RMRS OF ATTITUDE TRACKING ERRORS [RAD]

Test No.	Pitch control error	Yaw control error
Test 2A	0.0150	0.0250
Test 2B	0.0140	0.0247
Test 2C	0.0131	0.0218
Test 2D	0.0046	0.0151

ACKNOWLEDGEMENT

This work is partly supported by the JSPS Grants-in-Aid for Scientific Researches No. 22K14283, and the Nagamori Research Grants.

REFERENCES

[1] L. Abualigah, A. Diabat, P. Sumari, and A. H. Gandomi, "Applications, Deployments, and Integration of Internet of Drones (IoD): A Review," IEEE Sensors Journal, Vol. 21, Iss. 22, pp. 25532-25546, 2021.

[2] B-M. Nguyen, T. Kobayashi, K. Sekitani, M. Kawanishi, and T. Narikiyo, "Altitude Control of Quadcopters with Absolute Stability Analysis," IEEJ Journal of Industry Applications, Vol. 11, No. 4, pp. 562-572, 2022.

[3] R. Wang, C. Zhao, Y. Bai, W. Du, and J. Wang, "An Actuator Fault Detection and Reconstruction Scheme for Hex-Rotor Unmanned Aerial Vehicle," IEEE Access, Vol. 7, pp. 93937-93951, 2019.

[4] A. G. Rot, A. Hasan, and P. Manoonpong, "Robust Actuator Fault Diagnosis Algorithm for Autonomous Hexacopter UAVs," IFAC Paper OnLine, Vol. 53, No. 2, pp. 682-687, 2020.

[5] G. Ortiz-Torres, P. Castillo, P. D. J. Sorcia-Vazquez, J. Y. Rumbo-Morals, J. A. Brizuela-Mendoza, J. De la Cruz-Soto, and M. Martinez-Garcia, "Fault Estimation and Fault Tolerant Control Strategies Applied to VTOL Aerial Vehicles with Soft and Aggressive Actuator Faults," IEEE Access, Vol. 8, pp. 10649-10661, 2020.

[6] Y. Zhong, Y. Zhang, W. Zhang, J. Zuo, and H. Zhan, "Robust Actuator Fault Detection and Diagnosis for a Quadrotor UAV with External Disturbances," IEEE Access, Vol. 6, pp. 48169-48180, 2018.

[7] S. Zeghlache, A. Djerioui, L. Benyettou, T. Benslimane, H. Mekki, and A. Bouguerra, "Fault Tolerant Control for Modified Quadrotor Via Adaptive Type-2 Fuzzy Backstepping Subject to Actuator Faults," ISA Transactions, Vol. 95, pp. 330-345, 2019.

[8] A. Baldini, R. Felicetti, A. Freddi, S. Longhi, and A. Monteriu, "Actuator Fault Tolerant Control of Variable Pitch Quadrotor Vehicles," IFAC Papers OnLine, Vol. 53, Iss. 2, pp. 4095-4012, 2020.

[9] J. S. Souza, M. C. Bezerril, M. A. Silva, F. C. Veras, A. Lima-Filho, J. G. Ramos, and A. V. Brito, "Motor Speed Estimation and Failure Detection of a Small UAV Using Density of Maxima," Frontiers of Information Technology and Electronic Engineering, Vol. 22, No. 7, pp. 1002-1009, 2021.

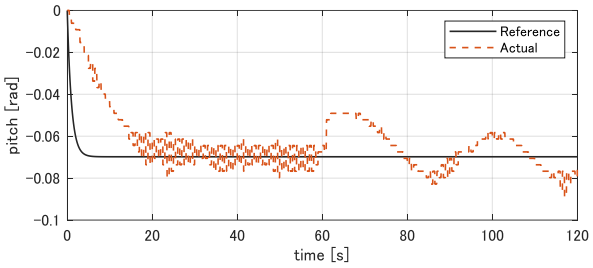

(a) Pitch

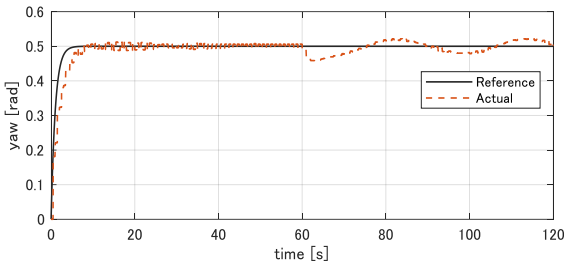

(b) Yaw

Fig. 12. Test 2A: Conventional control system.

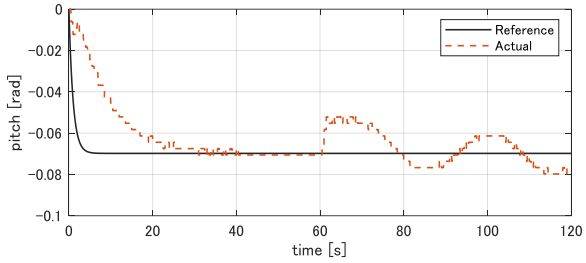

(a) Pitch

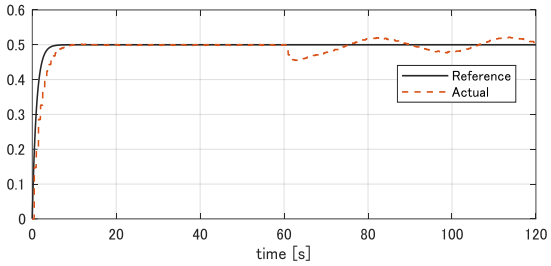

(b) Yaw

Fig. 13. Test 2B: Multirate feedback control system.

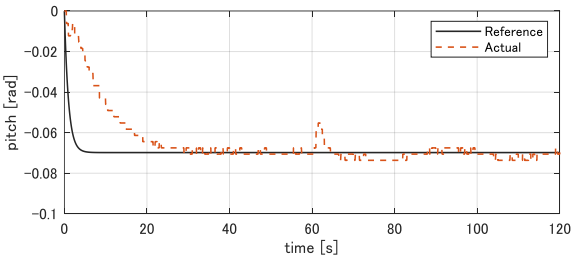

(a) Pitch

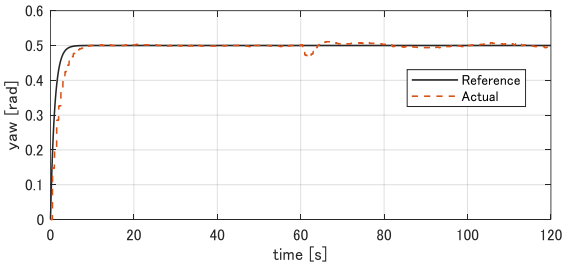

(b) Yaw

Fig. 14. Test 2C: Multi-rate feedback control system with LoE compensation

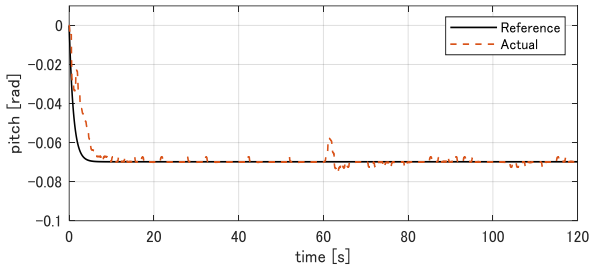

(a) Pitch

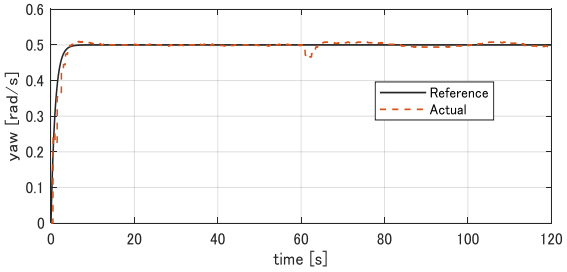

(b) Yaw

Fig. 15. Test 2D: Proposed multi-rate control system with LoE compensation and adaptive feedforward controller.

[10] R. C. Avram, X. Zhang, and J. Muse, "Quadrotor Actuator Fault Diagnosis and Accommodation Using Nonlinear Adaptive Estimators," IEEE Transactions on Control Systems Technology, Vol. 25, No. 6, pp. 2219-2226, 2017.

[11] H. Fujimoto and Bin Yao, "Multirate Adaptive Robust Control for Discrete-time Non-minimum Phase Systems and Application to Linear Motors," IEEE/ASME Transactions on Mechatronics, Vol. 10, No. 4, pp. 371-377, 2005.

[12] K. Ohno, H. Fujimoto, Y. Isaoka, and Y. Terada, "Adaptive Cutting Force Observer for Machine Tool Considering Stage Parameter Variation," IEEE International Conference on Mechatronics, pp. 1-6, 2021.

[13] B. -M. Nguyen, S. Hara and V. P. Tran, "A Multi-Agent Approach to Landing Speed Control with Angular Rate Stabilization for Multirotors," IEEE Vehicle Power and Propulsion Conference, pp. 1-6, 2022.

[14] B-M. Nguyen, W. Ohnishi, Y. Wang, H. Fujimoto, Y. Hori, K. Ito, et al., "Dual Rate Kalman Filter Considering Delayed Measurement and Its Application in Visual Servo", 13th IEEE International Workshop on Advanced Motion Control, pp. 494-499, 2014.

[15] K. J. Aström and B. Wittenmark, "Adaptive Control," Addition-Weslay Publishing Company, Second Edition, 1995.

[16] H. Fujimoto, K. Fuji, and N. Takahashi, "Traction and Yaw-rate Control of Electric Vehicle with Slip-ratio and Cornering Stiffness Estimation," American Control Conference, pp. 5742-5747, 2007.